Synchronization of a thermoacoustic oscillator by an external sound source

G. Penelet and T. Biwa

Citation: Am. J. Phys. **81**, 290 (2013); doi: 10.1119/1.4776189
View online: http://dx.doi.org/10.1119/1.4776189
View Table of Contents: http://ajp.aapt.org/resource/1/AJPIAS/v81/i4
Published by the American Association of Physics Teachers

Synchronization of a thermoacoustic oscillator by an external sound source

G. Penelet[a)]
LUNAM Université, Université du Maine, CNRS UMR 6613, Laboratoire d'Acoustique de l'Université du Maine, Avenue Olivier Messiaen, 72085 Le Mans Cedex 9, France

T. Biwa
Department of Mechanical Systems and Design, Tohoku University, 980-8579 Sendai, Japan

(Received 23 July 2012; accepted 29 December 2012)

Since the pioneering work of Christiaan Huygens on the sympathy of pendulum clocks, synchronization phenomena have been widely observed in nature and science. In this paper, we describe a simple experiment, with a thermoacoustic oscillator driven by a loudspeaker, which exhibits several aspects of synchronization. Both the synchronization region of leading order around the oscillator's natural frequency f_0 and regions of higher order (around $f_0/2$ and $f_0/3$) are measured as functions of the loudspeaker voltage and frequency. We also show that increasing the coupling between the loudspeaker and the oscillator gives rise under some circumstances to the death of self-sustained oscillations (quenching). Moreover, two additional set of experiments are performed: the first investigates a feedback loop in which the signal captured by the microphone is delivered to the loudspeaker through a phase-shifter; the second investigates the nontrivial interaction between the loudspeaker and the oscillator when the latter acts as a relaxation oscillator (spontaneous and periodic onset/damping of self-sustained oscillations). The experiment is easy to build and highly demonstrative; it might be of interest for classroom demonstrations or an instructional lab dealing with nonlinear dynamics.
[http://dx.doi.org/10.1119/1.4776189]

I. INTRODUCTION

Synchronization is the phenomenon in which a self-sustained oscillator changes its frequency when coupled to another system oscillating with different frequencies. It was first reported by Christiaan Huygens,[1,2] who observed that two pendulum clocks hanging from the same beam synchronized mutually—the frequency of each pendulum changed slightly in order that they swung in perfect harmony with opposite (anti-phase-locked) motions. Since the pioneering work of Huygens, synchronization has been observed or used advantageously in many fields of science,[3,4] including chemistry (e.g., the Belousov-Zhabotinsky reaction), physics (lasers), medicine (artificial pacemakers), biology (synchronization of fireflies and singing crickets), electronics engineering (synchronization of triode generators), and even in social life (a clapping audience). Research on this process is currently still active.[4,5]

Although synchronization is a well-known phenomenon, it is not widely appreciated. It can be understood within the common framework of nonlinear dynamics. When teaching this subject, it is helpful to have some demonstration devices that exhibit such phenomena as synchronization of a nonlinear oscillator by an external force, mutual synchronization of oscillators, chaotic synchronization, and so on. For example, one simple demonstration of mutual synchronization consists of two metronomes resting on a plate that sits on two soda cans.[7] In addition, the famous Van der Pol oscillator excited by an external periodic force[8] can nowadays be realized with operational amplifiers.[9]

Synchronization processes have also been studied in the field of acoustics. The mutual synchronization of organ pipes was studied more than a century ago by Lord Rayleigh[6] and has been revisited recently.[10,11] Rayleigh notably reported the quenching effect (or beating death[2]), which refers to the quasi-suppression of oscillations due to the nonlinear interaction of the oscillators. Organ pipes, brass, and reed musical instruments are excellent examples of self-sustained acoustic oscillators; another interesting example is the thermoacoustic oscillator, a modern version of the Sondhauss tube.[12] A thermoacoustic oscillator is basically composed of a gas column in a pipe partially filled with a stack of solid plates; the onset of thermoacoustic instability builds up when a critical temperature gradient is applied along the stack, and the frequency of self-sustained acoustic oscillations generally corresponds to the first resonance of the gas column.[13] This device has been extensively studied for the past three decades because it can be used as a new kind of thermodynamic engine,[14] but it is also interesting as an autonomous oscillator excited by heat.

Most research studies of thermoacoustic oscillators have dealt with their fundamental principles and optimization for energetic use,[15] but one can also find a few papers in which synchronization processes are considered.[16–20] Spoor and Swift[20] took advantage of the mutual synchronization of two thermoacoustic engines in order to cancel the vibrations of the pipes induced by high-amplitude acoustic waves. Yazaki *et al.*[16,17] reported that Taconis oscillations—thermoacoustic oscillations observed at cryogenic temperatures—exhibit synchronization and chaotic dynamics when forced by external oscillations. Müller and Lauterborn[18,19] made an experimental study of the thermoacoustic oscillator coupled through a small hole to an electrodynamic loudspeaker excited by a sinusoidal voltage with varying amplitude and frequency. Most of the work presented in the present paper is similar (and complementary) to that of Müller and Lauterborn, but the main motivation here is to present a simple apparatus that would be of interest for demonstration in classrooms. Our experimental device is the simplest thermoacoustic oscillator one can build, which requires only a

glass tube, a piece of ceramic catalyst, and a Nichrome wire, while the study of its interaction with an external oscillating force requires only a loudspeaker and basic instrumentation.

In the following, we examine the nonlinear interaction between a loudspeaker and a thermoacoustic oscillator. We vary both the driving amplitude (loudspeaker voltage) and the driving frequency, which allows us to draw so-called Arnold tongues.[4] The differences in the transition to synchronization for weak forcing (saddle-node bifurcation) and strong forcing (Hopf bifurcation) are highlighted. We also show that when the distance between the loudspeaker and the open end of the pipe is short, it is possible to observe the quenching process within a certain range of driving force and frequency. Experiments are also performed using a feedback loop between the microphone and the loudspeaker: the insertion of a phase-shifting circuit along this feedback loop allows the control of the amplitude of self-sustained acoustic waves,[21] including the possibility of beating death. Finally, we investigate the nonlinear interaction between the loudspeaker and the thermoacoustic oscillator when the latter acts as an *integrate-and-fire* oscillator;[4] this case corresponds to a specific regime for which periodic bursts of (instead of stable) self-sustained acoustic oscillations are generated spontaneously in the resonator. The external action of the loudspeaker leads not only to the synchronization but also to the stabilization of acoustic oscillations.

II. EXPERIMENTAL APPARATUS

The thermoacoustic oscillator considered here is the so-called *acoustic laser*,[22] which is very easy to build. A photograph of the complete apparatus is shown in Fig. 1(a). The system consists of a glass tube (length $L = 49$ cm, inner radius $r_i = 26$ mm, outer radius $r_e = 30$ mm), open at one end, and closed by a rigid plug at the other end. The core of the engine—the stack—is an open-cell porous cylinder (radius r_i, length $x_s = 48$ mm) that is inserted into the waveguide. This stack is made up of a 600 CPSI (cells per square inch) ceramic catalyst with numerous square channels of section $0.9\,\text{mm} \times 0.9\,\text{mm}$. In this device, imposing a large temperature gradient along the stack leads to the onset of self-sustained acoustic waves oscillating at the frequency f_0 of the most unstable acoustic mode (generally, $f_0 \approx c_0/4L$ where c_0 is the adiabatic sound speed at room temperature T_∞). As illustrated in Fig. 1(b), the side of the stack facing the plug is heated using an electrical resistance wire (Nichrome wire, 36 cm in length, 0.25 mm in diameter, resistivity 7 Ω/ft) regularly coiled through the stack end, and connected to a DC electrical power supply. Sound is captured using a 1/4-in. condenser microphone (model GRAS, type 40BP) flush-mounted through the plugged end of the resonator. Forced synchronization is achieved with a loudspeaker enclosure (Cabasse, type Brick M7) placed at a distance d from the open end of the tube. Data monitoring is accomplished using an oscilloscope and an audio spectrum analyzer, while both the oscillating pressure and loudspeaker voltage are recorded with a data acquisition card, as illustrated in Fig. 1(c).

The post-processing consists of calculating both the fast Fourier transform (FFT) and the Hilbert transform of the sampled data, which enables the computation of the analytic signals

$$p_{\text{ana}}(t) = p(t) + ip_H(t) = A_p(t)e^{i\Phi_p(t)}, \tag{1a}$$

$$U_{\text{ana}}(t) = U(t) + iU_H(t) = A_u(t)e^{i\Phi_u(t)} \tag{1b}$$

of both acoustic pressure $p(t)$ and loudspeaker voltage $U(t)$. Here, p_H and U_H stand for the Hilbert transforms of p and U, respectively. The relevant parameters that will be used in the following to analyze synchronization processes are the instantaneous phases $\Phi_{p,u}(t)$ and amplitudes $A_{p,u}(t)$.

III. MEASUREMENT OF THE ARNOLD TONGUES

The defining feature of synchronization is the variation of the natural frequency f_0 of the autonomous oscillator due to the action of an external periodic force with frequency f.

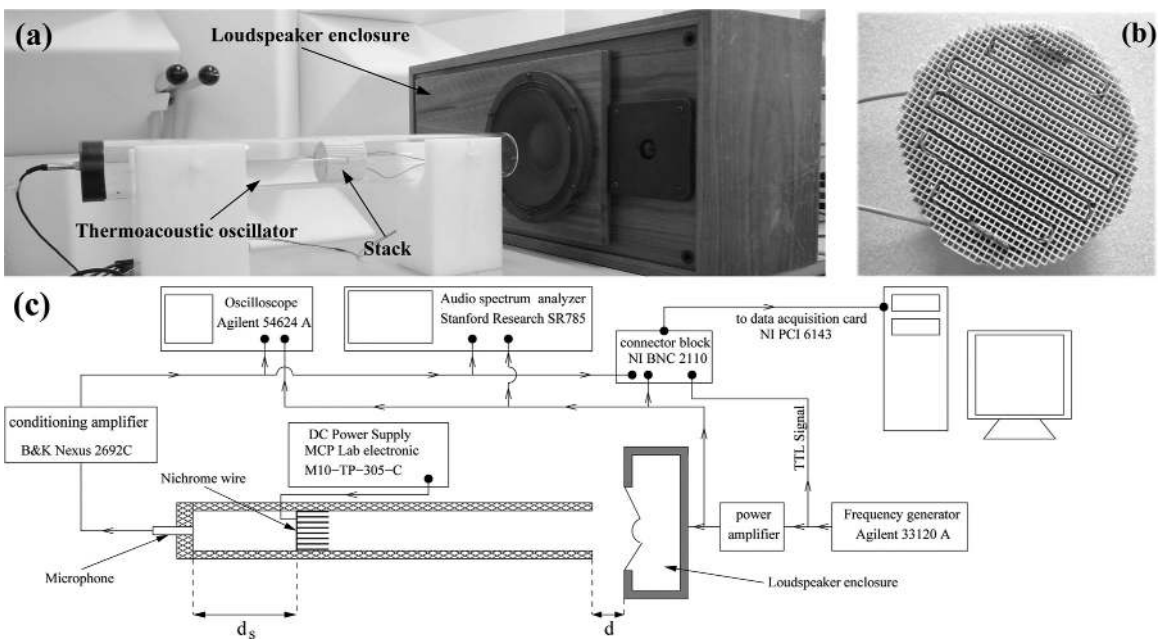

Fig. 1. Photographs of (a) the experimental setup and (b) the hot side of the stack. A schematic diagram of the complete experimental setup is shown in (c).

This process can occur when $f \approx f_0$ (synchronization of the order 1: 1) so that the natural frequency f_0 slips to the frequency f of the external force, but it can also be observed when the ratio of the two frequencies is close to a ratio m/n of integers. For example, synchronization of order 2:1 can be observed when $2f \approx f_0$ so that the frequency of the autonomous oscillator locks to 2 f. This occurrence of *frequency locking* depends on both the amplitude of the force and the frequency detuning $f - f_0$ (or more generally $nf - mf_0$). By varying these two parameters, it is then possible to measure the synchronization regions, which are now commonly called the Arnold tongues.

With the present device, it is very easy to change the coupling between the loudspeaker and the thermoacoustic engine by simply varying the distance d [see Fig. 1(c)]. It is also easy to change the position d_s of the stack along the resonator, which enables the control of the amplitude and the dynamics of thermoacoustic oscillations. We observed the higher order synchronizations of 3:1, 2:1, and 1:2, in addition to the 1:1 synchronization. In Fig. 2, the Arnold tongues obtained in experiments are plotted for three different cases in which both the coupling distance d and the stack position d_s are changed.

In order to obtain the above-mentioned Arnold tongues, the following experimental procedure was used. After having fixed the coupling distance d and the stack position d_s, all instruments are switched on (except for the frequency generator) and the power supplied to the Nichrome wire is fixed at $Q_0 = 22.6\,\mathrm{W}$ so that stable self-sustained thermoacoustic oscillations are generated in the waveguide at frequency f_0. After a time delay of about 30 min, the frequency generator is switched on and the Arnold tongues are measured by varying the forcing frequency f around f_0 (or around nf_0), and by gradually increasing the loudspeaker voltage. Data acquisition is performed using a sampling frequency f_s, which is exactly 30 times the forcing frequency (or $f_s = 30 \times nf$ in the case of higher-order Arnold tongues), and the number N of samples is chosen so that the frequency resolution f_s/N is less than 0.1 Hz. It is worth mentioning that the Arnold tongues that are plotted in Fig. 2 do not strictly correspond to the actual Arnold tongues. One reason for this is that only a finite number of operating points (f, U_{rms}) could be measured; another reason is that it is impossible to detect the exact bounds of the synchronization regions since an infinite time is required to cross the bound with an infinitely small detuning δf. For instance, we observed that for the device initially in a non-synchronous state, and after having changed the forcing frequency by $\delta f = 0.1\,\mathrm{Hz}$, the device could take more than 30 min before synchronization was attained. In the experiments, we chose $\delta f = 0.1\,\mathrm{Hz}$ as the lower limit of frequency variations, and we did not wait for more than 4 min before passing to a new operating point. The results depicted in Fig. 2 were obtained in a total time of more than 50 h from a total number of data files that exceeds 1400. Note that an improvement of the experimental protocol could consist in automatizing the experiments over several weeks.[11]

The results depicted in Fig. 2(a) were obtained when the stack was placed at a distance $d_s = 8\,\mathrm{cm}$ from the closed end of the resonator, while the distance d between its open end and the loudspeaker was fixed at 5 mm. In the absence of forcing, the frequency of self-sustained oscillations f_0 equals $172 \pm 0.05\,\mathrm{Hz}$ and the root-mean-square amplitude p_{rms} of acoustic pressure at the closed end of the resonator equals

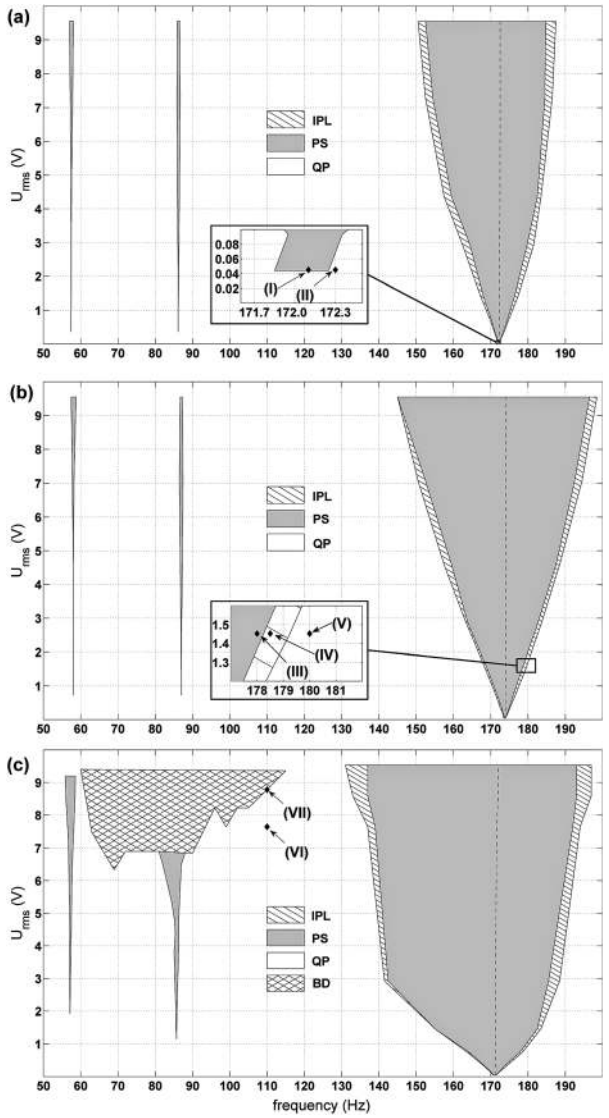

Fig. 2. Arnold tongues obtained in the experiments as a function of the driving frequency f and of the root-mean-square amplitude U_{rms} of the loudspeaker voltage for: (a) $d = 5\,\mathrm{mm}$, $d_s = 8\,\mathrm{cm}$; (b) $d = 5\,\mathrm{mm}$, $d_s = 19\,\mathrm{cm}$; and (c) $d = 1\,\mathrm{mm}$, $d_s = 8\,\mathrm{cm}$. The regions are labelled as follows: PS corresponds to perfect synchronization; QP corresponds to quasi-periodicity (loss of synchronization); IPL corresponds to imperfect phase locking, for which the signal looks quasi-periodic but the phase difference stays bounded; and BD corresponds to "beating death," for which the self-sustained oscillations are almost reduced to silence.

292 ± 5 Pa. Note that after more than 12 h of measurements in this device configuration, both the frequency and the amplitude of acoustic oscillations drifted slightly, to 172.6 Hz and 330 Pa, respectively, due to a gradual change of the temperature distribution in the thermoacoustic engine. (Similar variations of f_0 and p_{rms} have been observed in the other experiments.) The results depicted in Fig. 2(b) were obtained with $d_s = 19\,\mathrm{cm}$ and $d = 5\,\mathrm{mm}$; the initial values of f_0 and p_{rms} are 173.5 Hz and 350 Pa, respectively. From the analysis of the Arnold tongues in Figs. 2(a) and 2(b), it appears that the position of the stack impacts the width of the leading-order Arnold tongue, but the differences between the two sets of measurements are not very significant.

Some of the results depicted in Figs. 2(a) and 2(b) require additional explanations. Three different states are drawn in

the (f, U_{rms}) plane. The first state, denoted PS, corresponds to "perfect synchronization," for which the instantaneous phase of pressure oscillations locks to that of the oscillating force. The second state, denoted QP, corresponds to "quasi-periodicity," for which the thermoacoustic oscillator keeps its own natural frequency f_0. The last state, denoted IPL, corresponds to "imperfect phase locking," for which the instantaneous phase difference $\Psi(t) = \Phi_p(t) - \Phi_u(t)$ is not constant but stays bounded. These different states are explained in more detail below.

The transition from perfect synchronization to quasi-periodicity in the case of weak forcing is illustrated by different means in Fig. 3. The most obvious way of analyzing the results is to look at the acoustic pressure $p(t)$ together with its FFT amplitude $p(f)$; this is done in Fig. 3(a) for two operating points, referred to as (I) and (II) in Fig. 2(a). The

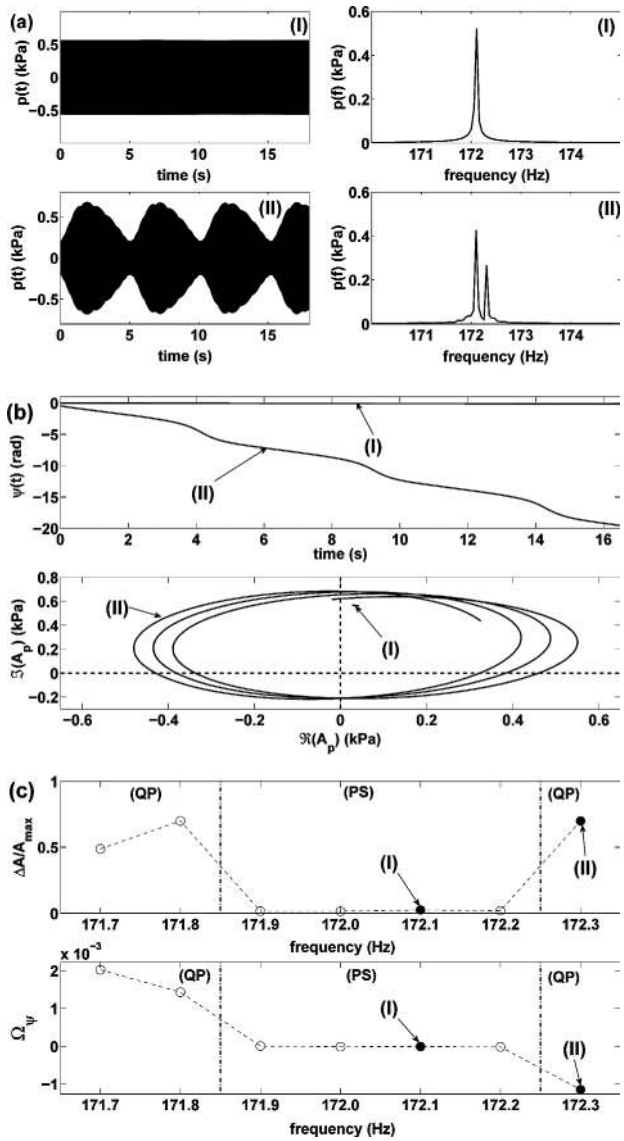

Fig. 3. Transition to synchronization in the case of weak forcing ($U_{\mathrm{rms}} \approx 40$ mV): (a) acoustic pressure $p(t)$ and frequency spectra $p(f)$ measured for the two operating points labeled (I) and (II) in Fig. 2(a); (b) time evolution of the instantaneous phase difference $\Psi(t) = \Phi_p(t) - \Phi_u(t)$, and time evolution of the real part $\Re(A_p)$ of the instantaneous amplitude as a function of its imaginary part $\Im(A_p)$ in the frame rotating at angular frequency $\omega = 2\pi f$; (c) normalized amplitude modulation $\Delta A/A_{\max}$, and normalized time-average phase difference Ω_Ψ, as functions of the frequency detuning.

operating point (I) is within the synchronization region; the pressure signal does not exhibit any amplitude modulation, and the frequency of self-sustained oscillations matches the forcing frequency $f = 172.1$ Hz. The operating point (II) is outside the synchronization region; the pressure signal exhibits large amplitude modulations while two distinct peaks are clearly visible in the spectrum.

There also exists other ways of analyzing the raw data, which are illustrated in Fig. 3(b) for the two operating points (I) and (II). The first is to plot the instantaneous phase difference $\Psi(t)$, which should be constant in the case of perfect synchronization and unbounded in the case of quasi-periodicity.[4] The second is to plot the data in some kind of a phase space, by tracing the real part $\Re(A_p)$ of the instantaneous amplitude of the acoustic pressure as a function of its imaginary part $\Im(A_p)$ in the frame rotating at angular frequency $\omega = 2\pi f$. As illustrated in Fig. 3(b), the phase difference $\Psi(t)$ of the operating point (I) is constant while that of point (II) gradually decreases with time; in the phase space, point (I) is a fixed point while point (II) draws an elliptic limit cycle.

Finally, it is also interesting to look at the transition to synchronization as a function of frequency detuning, for a fixed forcing amplitude U_{rms}. In Fig. 3(c), the normalized amplitude modulation $\Delta A/A_{\max}$ and the normalized time-average phase difference Ω_Ψ are plotted as a function of the forcing frequency. These two parameters are defined as

$$\frac{\Delta A}{A_{\max}} = \frac{\max\left(|A_p(t)|\right) - \min\left(|A_p(t)|\right)}{\max\left(|A_p(t)|\right)} \tag{2}$$

and

$$\Omega_\Psi = \frac{1}{T}\int_0^T \frac{\Psi(t)}{2\pi f_0}\,dt, \tag{3}$$

where T represents the total duration of data acquisition. The results depicted in Fig. 3(c) show that the loss of synchronization, represented as vertical dotted lines, corresponds to the appearance of beating ($\Delta A \neq 0$), while the phase becomes unbounded ($\Omega_\Psi \neq 0$). Note, however, that the frequency increment (or decrement) δf is not sufficient here—increasing the number of data points would allow one to check that the evolution of Ω_Ψ with frequency detuning outside synchronization obeys a square-root law, which is typical of a saddle-node bifurcation expected by theory in the case of weak-forcing.[23]

The transition from perfect synchronization to quasi-periodicity in the case of strong forcing is illustrated in Fig. 4, using the same representations as those of Fig. 3. The driving voltage is much higher ($U_{\mathrm{rms}} \approx 1.45$ V), which leads to a more complicated transition. The operating point referred to as (IV) is particularly interesting. According to Fig. 2(b), this point is within the region called "IPL," but in Fig. 4(a), the motion of the forced nonlinear oscillator looks quasi-periodic. However, it appears from the analysis of $\Psi(t)$ in Fig. 4(b) that the instantaneous phase difference $\Psi(t)$ is not constant but bounded, which means that there is an *imperfect* phase locking. In other words, the nonlinear interaction of both oscillators still corresponds to synchronization, since the frequency of the thermoacoustic oscillator is still controlled by that of the external force. In the phase space diagram, the difference between imperfect phase locking and quasi-periodicity is less obvious because both of the operating points (IV) and (V) correspond to limit cycles, but

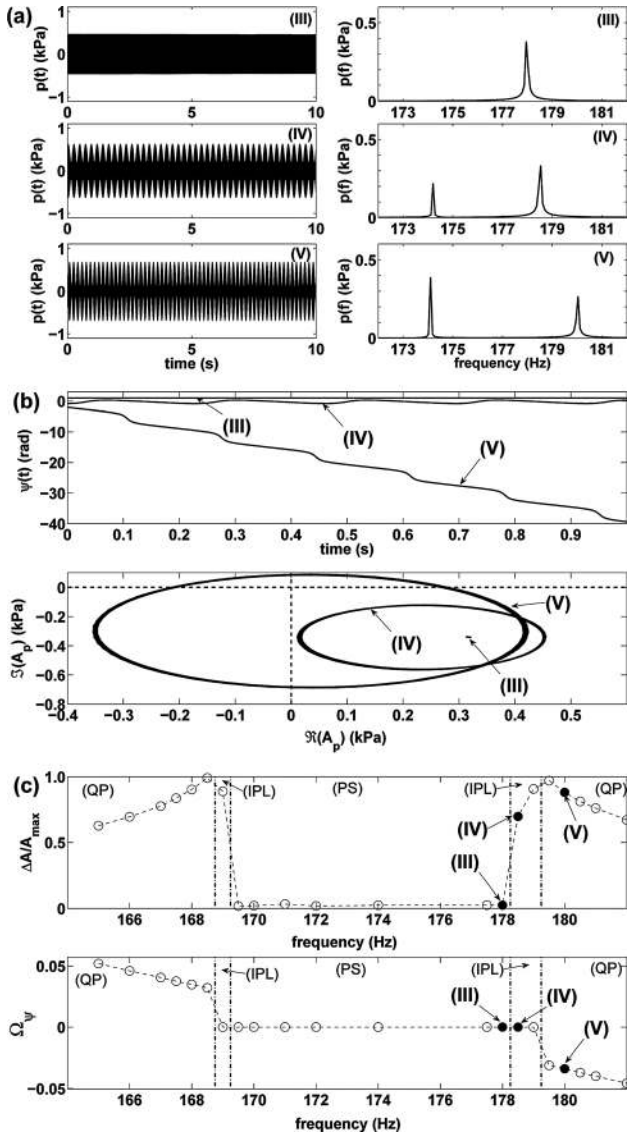

Fig. 4. Transition to synchronization in the case of strong forcing ($U_{\rm rms} \approx 1.45$ V): (a) acoustic pressure $p(t)$ and frequency spectra $p(f)$ measured for the three operating points (III), (IV), and (V) in Fig. 2(b); (b) time evolution of the instantaneous phase difference and representation in phase space of the operating points (III) to (V); (c) normalized amplitude modulation and normalized time-average phase difference as functions of the frequency detuning.

the limit cycle of point (IV) does not envelop the origin.[23] Finally, from the analysis of Fig. 4(c), the transition between perfect synchronization and imperfect phase locking, which operates through a Hopf bifurcation,[23] is clearly visible and corresponds to the bound for which amplitude modulation appears while the time-average phase difference is still zero.

The results depicted in Fig. 2(c) were obtained with the stack placed at a distance $d_s = 8$ cm from the closed end of the resonator, while the distance d between its open end and the loudspeaker was decreased to 1 mm. In the absence of forcing we have $f_0 \approx 171.3$ Hz and $p_{\rm rms} \approx 230$ Pa. The results exhibit significant differences from those of Figs. 2(a) and 2(b), which means that changing the distance d impacts the nonlinear coupling between the loudspeaker and the thermoacoustic oscillator. First, the Arnold tongues are significantly larger, and the leading-order Arnold tongue becomes asymmetric (it is not centered around f_0 for large forcing). Second, a new region appears around the synchronization region 2:1, which is labeled BD for "beating death." This effect is related to the fact that self-sustained oscillations are almost reduced to silence, and is illustrated in Fig. 5. In Fig. 5(a), the difference between the amplitude of the spectral component at frequency $f_0 \approx 171.3$ Hz and the one at frequency $f = 110$ Hz is plotted as a function of the driving voltage $U_{\rm rms}$. This difference, $L_p(f) - L_p(f_0)$, is plotted in terms of sound pressure levels, defined as $L_p = 20\log_{10}(p/p_0)$, where $p_0 = 20\,\mu$Pa. From the analysis of Fig. 5(a), we can clearly see that a gradual increase of the driving voltage $U_{\rm rms}$ leads above some threshold value to the abrupt extinction of self-sustained oscillations, which are almost reduced to silence compared to the forced oscillation. When drawing the BD zone in Fig. 2(c) we had to choose arbitrarily a threshold value of $L_p(f) - L_p(f_0) = 30$ dB, above which it is considered that beating death occurs. In Fig. 5(b), the frequency spectra of acoustic pressure are plotted for two operating points labeled (VI) and (VII) in Fig. 2(c). Point (VI) is within the quasi-periodicity region and its frequency spectrum shows both frequencies f and f_0 together with their linear combinations. Point (VII) is within the beating death region and its frequency spectrum shows that the spectral component f_0 is almost 50 dB lower than the one at frequency f, while all of the combination frequencies have disappeared.

The results depicted in Fig. 2(c) are similar to those obtained by Müller and Lauterborn[18] because we observed both n:1 synchronization and beating death in the frequency range around $f_0/2$. However, the shape of the Arnold tongues, or the conditions by which quenching is observed, are very different from those obtained in Ref. 18; this might be due to the fact that both the thermoacoustic engine and the coupling with the loudspeaker are different in the two studies.

IV. PHENOMENA IN ADDITION TO SYNCHRONIZATION

Apart from the measurement of the Arnold tongues, some further interesting experiments are possible with this simple thermoacoustic oscillator. Here, we describe two such experiments.

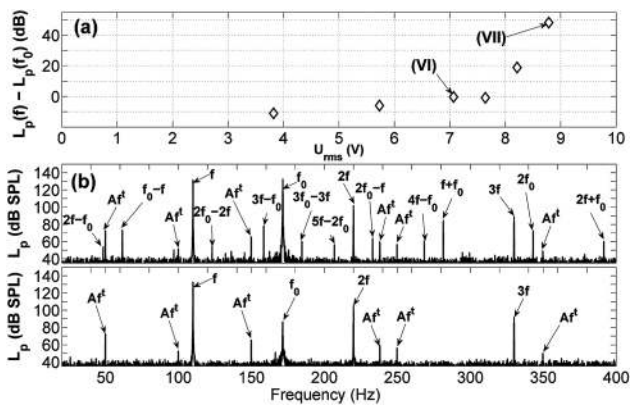

Fig. 5. Illustration of beating death in the case $f = 110$ Hz. (a) Measured difference between the sound pressure level $L_p(f)$ due to forcing, and the sound pressure level $L_p(f_0)$ due to self-sustained oscillations, as a function of the driving voltage $U_{\rm rms}$. (b) Frequency spectra corresponding to the operating points labeled (VI) and (VII) in Fig. 2(c). Note that the peaks labeled Af' correspond to measurement "artifacts" related to electromagnetic interference; these peaks are located at the electrical network frequency (50 Hz) and its harmonics, except for a peak at $f \approx 238$ Hz.

A. Feedback loop

Figure 6 shows the experimental setup for investigation of a feedback loop. In this experiment, illustrated in Fig. 6(a), the loudspeaker is no longer excited by the frequency generator but is instead excited by the signal captured by the microphone itself and amplified through the audio amplifier. Furthermore, a simple phase-shifting circuit[25] is inserted along the feedback loop and the effect of the assigned phase shift between the loudspeaker and the microphone on the self-sustained oscillations is investigated. The position of the stack is fixed at $d_s = 8$ cm, the coupling distance d is fixed at 1 mm, and the power Q_0 supplied to the Nichrome wire is 23 W. This kind of experiment has also been conducted by Müller and Lauterborn,[18] where the phase-shifting circuit was replaced by a multi-effects processor imposing an assigned time delay (instead of a phase shift). However, they did not succeed in initiating self-sustained thermoacoustic oscillations in their experiments.

In Fig. 6(b), the steady-state acoustic pressure is plotted as a function of the phase difference between the pressure measured by the microphone and the electrical voltage applied to the loudspeaker. This pressure is plotted for different values of the voltage gain $G = U_{out}/U_{in}$ [see Fig. 6(a)] monitored by the potentiometer of the audio amplifier. Note that the phase shift cannot be accurately adjusted in our experiments since it is set manually using a potentiometer. Moreover, we could only shift the phase between 0 and $3\pi/2$ using this phase shifter. When the voltage gain is set to zero (no feedback loop), the thermoacoustic oscillator sings with a frequency $f_0 \approx 171.7$ Hz. When the voltage gain is set to nonzero values, self-sustained oscillations take place within a certain range of the assigned phase shift, and the maximum value of the steady-state acoustic pressure is reached for $\phi_p - \phi_u \approx \pi/2$. This observation is consistent with our expectations since the acoustic oscillations at the open end of the waveguide should be roughly $\pi/2$ out of phase with those at the closed end of the waveguide. (Note also that the loudspeaker itself induces a small phase shift that depends on frequency.) Moreover, if the voltage gain is increased, the steady-state acoustic pressure is increased but the range of phase shift along which self-sustained oscillations can be observed decreases. For instance, when the voltage gain is fixed to 30×10^{-2}, self-sustained oscillations are quenched by the loudspeaker as soon as $\phi_p - \phi_u$ exceeds 240°. We did not conduct experiments for larger values of G because significant distortion was induced in the signals.

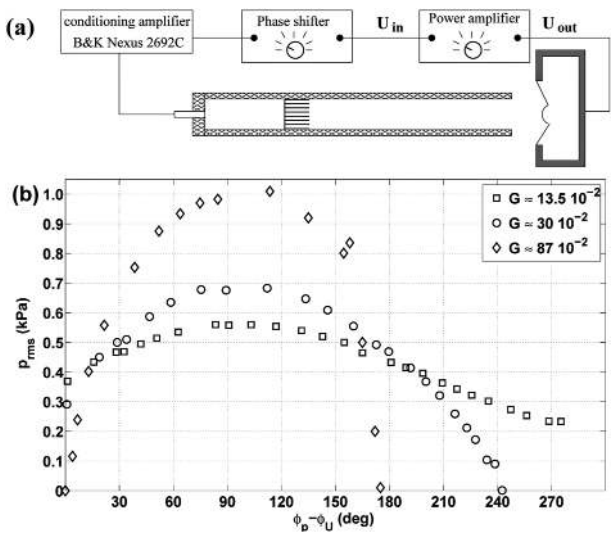

Fig. 6. Effect of a feedback loop. (a) Sketch of the experimental setup. (b) Steady-state acoustic pressure p_{rms} as a function of the assigned phase shift between the loudspeaker and the microphone signals, for different values of the voltage gain $G = U_{\mathrm{out}}/U_{\mathrm{in}}$, where U_{in} and U_{out} refer to the voltages at the input and the output of the audio power amplifier, respectively.

B. Synchronization in a relaxation regime

The thermoacoustic oscillator can also operate as a relaxation oscillator. When the stack is placed closer to the open end of the resonator and when the heater power supply is fixed at some value slightly above threshold, the amplitude of self-sustained acoustic oscillations is not stable; instead one can observe a spontaneous and periodic onset and damping of thermoacoustic instability.[24] The physical mechanisms that give rise to this kind of "integrate and fire" regime are not clearly understood, but it seems that this effect is due to a competition between the thermoacoustic amplification process induced by heating and the reciprocal effect of acoustic oscillations (thermoacoustic heat transport along the stack, acoustic streaming), which tend to decrease the assigned temperature gradient. In the experiment described below, the effect of external forcing by the loudspeaker is investigated under this particular regime.

The experimental setup is the same as the one of Fig. 1(c), but the stack is placed at a distance $d_s = 25$ cm from the rigid end of the resonator, while the coupling distance d is fixed at 4 cm and the power supplied to the Nichrome wire is fixed at $Q_0 = 24.5$ W. If the loudspeaker is switched off ($U_{\mathrm{rms}} = 0$, see Fig. 7), an integrate-and-fire regime of wave amplitude evolution takes place with a period of about 40 to 50 s. The frequency of self-sustained oscillations is around $f_0 \approx 177.1$ Hz, but this frequency actually varies during the process of wave amplification within each burst. For all of the experiments presented in Fig. 7, the forcing frequency f is set to 176.9 Hz (which differs slightly from f_0) and the nonlinear interaction between the loudspeaker and the thermoacoustic oscillator is investigated as a function of the driving voltage U_{rms}. Note that the loudspeaker is systematically switched on at time $t = 100$ s and it is switched off (except in the last case) at time $t = 150$ s. For very weak forcing ($U_{\mathrm{rms}} = 4$ mV), the spontaneous generation of periodic bursts is not disrupted by the forcing. However, self-sustained oscillations do not vanish completely between two bursts; instead a quasi-periodic regime of oscillations takes place. For intermediate amplitudes of loudspeaker voltage ($U_{\mathrm{rms}} = 10$ mV and $U_{\mathrm{rms}} = 105$ mV), the forcing impacts the integrate-and-fire regime of wave amplitude evolution—as soon as the loudspeaker is switched on, large amplitude modulations are clearly visible. Moreover, as soon as the loudspeaker is switched off, these modulations are quickly damped and the integrate-and-fire regime takes place once again. It is, however, worth noting that some additional time is required before the occurrence of a new regime of periodic bursts. This additional relaxation time increases with the amplitude of forcing, and this is due to the fact that external forcing also disrupts the evolution of the temperature field: heat must be diffused through the device before a new integrate-and-fire regime is attained. Finally, for larger amplitudes of the loudspeaker voltage ($U_{\mathrm{rms}} = 175$ mV and $U_{\mathrm{rms}} = 380$ mV), a new kind of nonlinear interaction is observed. As soon as the loudspeaker is switched on large

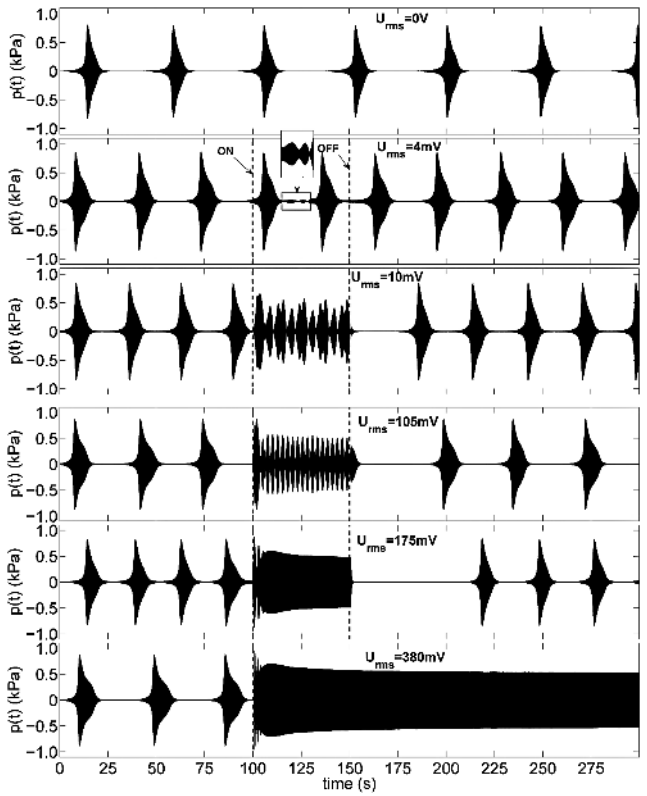

Fig. 7. Synchronization in a relaxation regime. The stack position is fixed at $d_s = 25$ cm while the coupling distance $d = 4$ cm; the heater power supply Q_0 is fixed at 24.5 W so that a spontaneous and periodic onset/damping of self-sustained oscillations takes place. From the upper graph to the lower graph, the effect of external forcing (frequency $f = 176.9$ Hz) on the dynamics of wave amplitude evolution is investigated with an increasing loudspeaker voltage U_{rms}. Except for the first (no forcing) and the last graph, the loudspeaker is switched on at time $t = 100$ s and switched off at time $t = 150$ s.

modulations of the acoustic pressure are generated, though they are quickly damped; this corresponds to the transition to synchronization, for which the natural frequency of the thermoacoustic oscillator gradually shifts down to the external frequency f. Furthermore, a less obvious process of wave amplitude stabilization by external forcing is also observed—the spontaneous generation of periodic bursts disappears, and instead stable acoustic oscillations occur. Note that if the loudspeaker is switched off ($U_{\text{rms}} = 175$ mV), the thermoacoustic oscillator goes back to its integrate-and-fire regime, but if the external forcing is maintained ($U_{\text{rms}} = 380$ mV), then acoustic oscillations stabilize to a finite amplitude. The results depicted in Fig. 7 could be partially interpreted by arguing that when periodic bursts of thermoacoustic oscillations are spontaneously generated, the nonlinear oscillator has two unstable states, one without oscillations and the other with finite-amplitude oscillations. Because of this behavior, the device switches alternately between the two states; however, a weak external force modifies this regime and makes one state more stable than the other.

V. CONCLUSION

We have described a simple apparatus that exhibits, via sound, several aspects of synchronization phenomena. The results presented in this paper do not constitute a complete investigation and additional processes could be explored, including the effect of a non-sinusoidal but periodic driving force or even an aperiodic force.[26] A deeper analysis of the experimental data would also require the use of standard tests in nonlinear dynamics such as calculation of the embedding dimension and of the Lyapunov exponents.[4,19] It is also challenging to find a simple model able to reproduce qualitatively the experimental results obtained above. Finally, it would be interesting to investigate the mutual synchronization of two thermoacoustic oscillators placed face to face, adjusting the frequency by replacing the rigid end with a sliding piston.

ACKNOWLEDGMENTS

The authors would like to thank the scientific council of the Université du Maine, for having provided a one-month invited professor position to Dr. Biwa. This opportunity allowed us to initiate this study.

[a]Electronic mail: guillaume.penelet@univ-lemans.fr

[1]C. Huygens, *Oeuvres Completes de Christiaan Huygens*, edited by M. Nijhoff (Société Hollandaise des Sciences, 1893).
[2]B. Bennett, M. F. Schatz, H. Rockwood, and K. Wisenfeld, "Huygens' clocks," Proc. R. Soc. London Ser. A **458**, 563–579 (2002).
[3]I. I. Blekhman, *Synchronization in Science and Technology* (ASME, New York, 1988).
[4]A. Pikovsky, M. Rosenblum, and J. Kurths, *Synchronization: A Universal Concept in Nonlinear Science* (Springer, Berlin, 2001).
[5]R. C. Hilborn and N. B. Tufillaro, "Resource Letter: ND-1: Nonlinear dynamics," Am. J. Phys. **65**, 822–834 (1997).
[6]J. W. Strutt (Lord Rayleigh), *The Theory of Sound* (Dover, New York, 1945).
[7]J. Pantaleone, "Synchronization of metronomes," Am. J. Phys. **70**, 992–1000 (2002).
[8]B. Van der Pol and J. Van der Mark, "Frequency demultiplication," Nature **120**, 363–364 (1927).
[9]G. Qin, D. Gong, R. Li, and X. Wen, "Rich bifurcation behavior of the driven Van der Pol oscillator," Phys. Lett. A **141**, 412–416 (1989).
[10]M. Abel, S. Bergweiler, and R. Gerhard-Multhaupt, "Synchronization of organ pipes: Experimental observations and modeling," J. Acoust. Soc. Am. **119**, 2467–2475 (2006).
[11]M. Abel, K. Ahnert, and S. Bergweiler, "Synchronization of sound sources," Phys. Rev. Lett. **103**, 114301-1–4 (2009).
[12]C. Sondhauss, "Über die Schallschwingungen der luft in erhitzten Glassröhren und in gedeckten Pfeifen von ungleicher Weite," Ann. Phys. (Leipzig) **79**, 1 (1850).
[13]For a simple example of how the critical temperature gradient depends on the working fluid, see D. Noda and Y. Ueda, "A thermoacoustic oscillator powered by vaporized water and ethanol," Am. J. Phys. **81**(2), 124–126 (2013).
[14]G. W. Swift, *Thermoacoustics: A Unifying Perspective for Some Engines and Refrigerators* (Acoustical Society of America, 2001).
[15]S. L. Garrett, "Resource Letter: TA-1: Thermoacoustic engines and refrigerators," Am. J. Phys. **72**, 11–17 (2004).
[16]T. Yazaki, S. Sugioka, F. Mizutani, and H. Mamada, "Nonlinear dynamics of a forced thermoacoustic oscillation," Phys. Rev. Lett. **64**, 2515–2518 (1990).
[17]T. Yazaki, "Experimental observation of thermoacoustic turbulence and universal properties at the quasiperiodic transition to chaos," Phys. Rev. E **48**, 1806–1818 (1993).
[18]G. Müller and W. Lauterborn, "Experiments with the thermoacoustic oscillator physical and musical," in *Proceedings International Symposium of Musical Acoustics*, Le Normont, Dourdan, France, 1995, pp. 178–183.
[19]W. Lauterborn, "Nonlinear dynamics in acoustics," Acta Acust. United Acust. **82**, Suppl. 1, S46–S55 (1996).
[20]P. S. Spoor and G. W. Swift, "The Huygens entrainment phenomenon and thermoacoustic engines," J. Acoust. Soc. Am. **108**, 588–599 (2000).
[21]C. Desjouy, G. Penelet, and P. Lotton, "Active control of thermoacoustic amplification in an annular engine," J. Appl. Phys. **108**, 114904-1–7 (2010).

[22]S. L. Garrett and R. L. Chen, "Build an acoustic laser," Echoes **10**(3), 4–5 (2000).
[23]A. S. Pikovsky, M. G. Rosenblum, and J. Kurths, "Phase synchronization in regular and chaotic systems," Int. Journ. Bifurc. Chaos **10**, 2291–2306 (2000).
[24]G. Penelet, M. Guedra, V. Gusev, and T. Devaux, "Simplified account of Rayleigh streaming for the description of nonlinear processes leading to steady state sound in thermoacoustic engines," Int. J. Heat Mass Transfer **55**, 6042–6053 (2012).
[25]J. S. Lopes, A. A. Melo, and V. S. Oliveira, "A simple phase shifting circuit," Phys. Educ. **17**, 238–240 (1982).
[26]R. V. Jensen, "Synchronization of driven nonlinear oscillators," Am. J. Phys. **70**, 607–619 (2002).

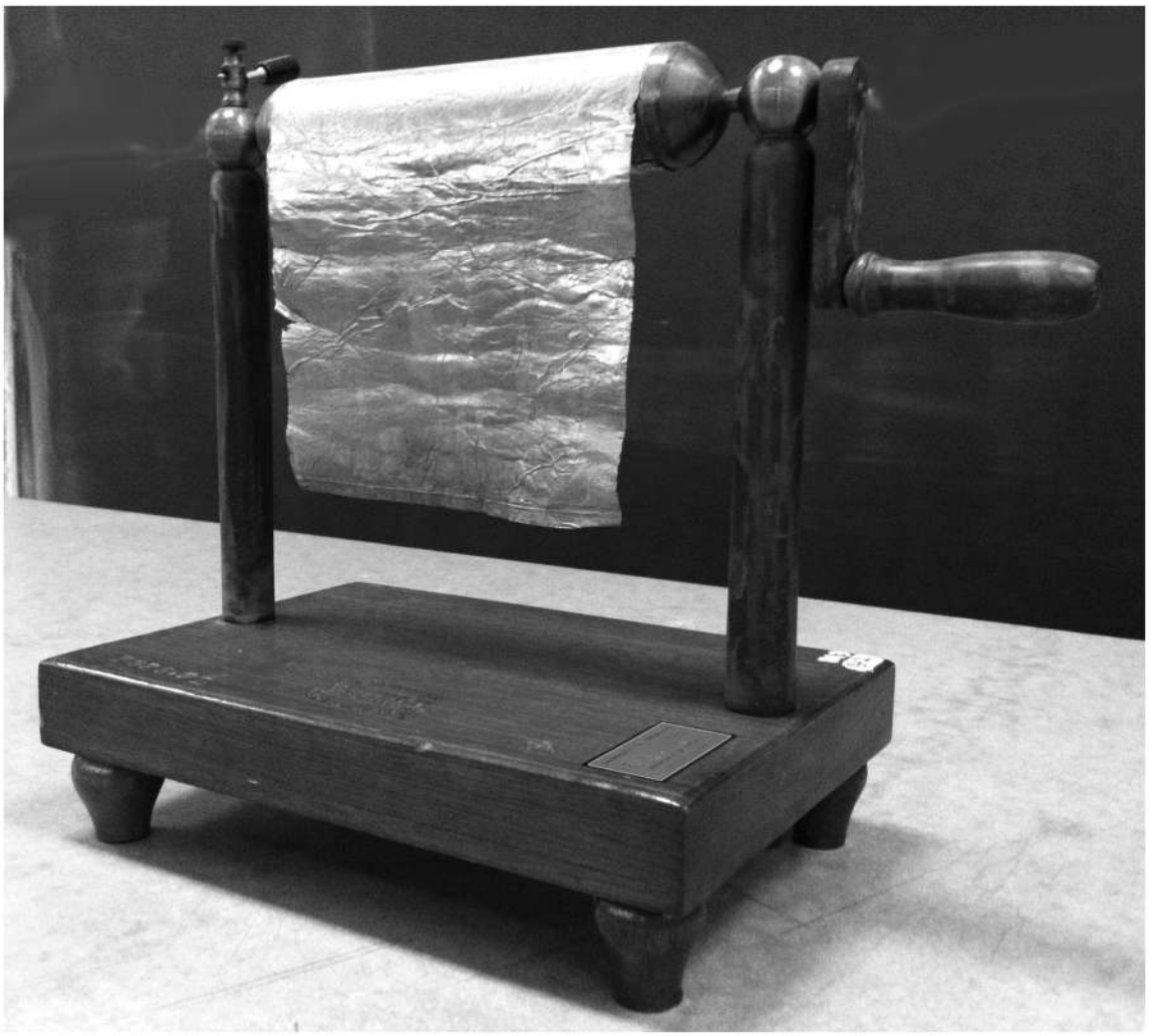

The Variable-Area Capacitor

From Ganot's *Physics*, 1883 edition, pp. 654–655: "A charge is imparted to the cylinder, by which a certain divergence [of an attached electroscope] is produced. On unrolling the tin-foil this divergence gradually diminishes, and increases as it is again rolled up. The quantity of electricity remaining the same, the electrical force [voltage] on each unit of surface, is thereby less as the surface is greater." Today we would say that since Q = CV is a constant, increasing C by unrolling the tinfoil will decrease V. This demonstration apparatus is at the University of Colorado. (Notes by Thomas B. Greenslade, Jr., Kenyon College; photograph by Michael Thomason, University of Colorado)